International Journal of Science Engineering and Advance Technology

Dc-Bus Voltage Control With A Three-Phase Bidirectional Inverter For Dc Distribution Systems

Venkata Manikanta Guttula[1], Mr.B,D.S.Prasad[2]
[1]PG Scholar, Pydah College of Engineering, Kakinada, AP, India.
[2]Assistant Professor, Pydah College of Engineering, Kakinada, AP, India.

***Abstract*—In this paper a new energy management system has been proposed for three-phase bidirectional inverter with dc-bus voltage control. The advantage of this bidirectional inverter is that it can operate in both grid connection and rectification modes with power factor correction. The proposed control system take into account dc-bus capacitance and control dc-bus voltage to track a linear relationship between the dc-bus voltage and inverter inductor current. The inverter tunes the dc-bus voltage every line cycle, which can reduce the frequency of operation-mode change and current distortion. With the increase in the demand of renewable energy sources, placed important role in distributed systems. In this paper battery storage system has been proposed with DG system. Battery storage system will give additional support to the DG system and also helps in controlling the DC bus voltage. The simulation results have been presented using MATLAB/SIMULINK software. The simulation results validated for the rectification mode with battery storage. This system will improve the performance of the DG system.**

***Index Terms*—Bidirectional inverter, capacitance estimation, dc distribution system, dc-bus voltage control, grid connection, rectification**

I. INTRODUCTION

In an ac-bus system, the maximum power point tracker (MPPT) will draw maximum power from photovoltaic (PV) arrays and inject the power into ac bus or ac grid through an inverter. For a typical offline application, such as electronic ballast, personal computer, or variable speed appliance, it usually has a rectifier, a power factor corrector (PFC), and a dc/dc or dc/ac converter to supply the loads. However, this ac system leads to high power conversion loss. Thus, the concept of "dc grid" or "dc distribution" system has been presented recently, and the system configuration is illustrated in Fig. 1(b). It can be calculated that the power conversion efficiency in the ac-bus system is less than that in the dc-bus system about 8%. In addition, the dc-bus system can also save one rectifier and one PFC, saving component cost around 25%. Therefore, the dc distribution system is feasible in renewable energy applications.

The dc distribution system requires a dc-bus voltage control to balance the power flow among PV panels, dc loads, and ac grid. When the overall PV power is higher than the dc load power, the bidirectional inverter, as shown in Fig. 1(b), needs to sell power to ac grid, which is often defined as grid-connection mode. On the contrary, the inverter will buy power from ac grid, which is a rectification, namely "rectification mode." Moreover, since in a dc distribution system, the dc-bus voltage is sensitive to step load changes, the control of dc-bus voltage is more critical than that in a grid-connected inverter system. In the past studies, the voltage control based on gain scheduling was presented, which use a droop concept to design proper dc gain. Moreover, some attempts combing the gain-scheduling with fuzzy control were also discussed, which incorporate fuzzy control and adjust dc voltage reference to balance power flow.

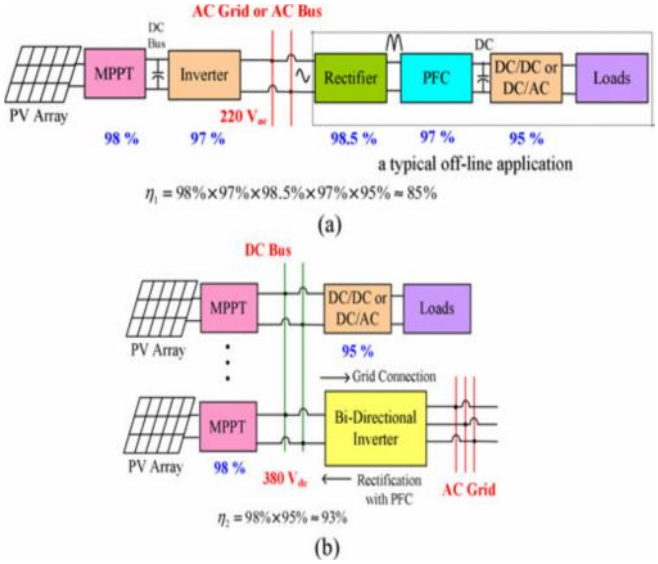

Fig. 1 Conceptual configurations of (a) an ac-bus system and (b) a dc distribution system

Then, other dc-bus voltage controls, such as robust, adaptive, and hybrid control to enhance system stability were reported. However, a dc distribution system requires a power management scheme to improve system availability; that is, it is allowed to have a certain range of dc-bus voltage variation for both grid-connection and rectification modes. When the system is operated in grid-connection mode, it needs a higher dc-bus voltage to prevent dramatic voltage drop below the lower bound due to a step dc load increase. On the contrary, it requires a lower dc-bus voltage to extend the range of voltage swing in rectification mode. In the literature, there are some power flow controls for dc distribution system with constant-power loads, such as general dc/dc converters, which behave with negative dynamic impedance. The loads with negative dynamic impedance will intend to regulate their input power under dc-bus voltage variation.

This effect can help the proposed control approach to stabilize the dc-bus voltage regulation. Moreover, the approaches for achieving fast dc-bus voltage dynamics were focused on the systems without dc loads, while there is no control for the bidirectional inverter systems with fast dc load variation. In our previous research, a digital controlled 10-kVA 3φ bidirectional inverter with wide inductance variation has been designed and implemented. Based on its configuration, this paper presents two dc-bus voltage regulation approaches, one line-cycle regulation approach (OLCRA) and one-sixth line-cycle regulation approach (OSLCRA), which are based on a linear power management scheme. They are chosen by considering that the dc-bus capacitance should be large enough (typically >4000 μF) to extend the hold-up time, and a short time interval does not vary the dc-bus voltage significantly even under high power change. Moreover, the OSLCRA is chosen for that the control laws for each region are changed every one-sixth line cycle, and the complexity of firmware programming can be reduced. The OLCRA is enacting for light load change while the OSLCRA is for heavy load change. The control laws of the two approaches require the information of dc-bus capacitance. It needs to determine the total capacitance on the dc bus. In a dc distribution system, dc loads or dc products having electrolytic capacitors are not desired to prevent inrush current.

The capacitors are installed in the inverter or in a separate box, and dc-bus capacitance estimation is only required at the start-up of the system operation. Several methods to estimate capacitance have been presented, where a dc-bus capacitance estimation method for ac/dc/ac pulse width modulation converter systems can determine the capacitance online with voltage injection. In this paper, an online capacitance estimation method with a capacitor pre-charging circuit at the system start-up is presented, which does not need extra inverter input current feedbacks. The proposed two control approaches can reduce the frequency of operation-mode change and current distortion significantly. In addition, they can improve the availability of the dc distribution system without increasing dc-bus capacitance.

II. DETERMINATION OF CAPACITOR SIZE AND CAPACITANCE ESTIMATION

The proposed system design is based on the power ratings of renewable sources, storage elements, dc load requirements, and the bidirectional inverter. The size of capacitors will affect the dc-bus voltage ripple and hold-up time. Thus, it needs to determine its size first, and then estimate the total capacitance online because of its tolerance.

A. Determination of Capacitor Size

In determining the capacitor size for the system, two major aspects are considered: dc-bus voltage ripple and energy-storage capability.

1) DC-Bus Voltage Ripple: By neglecting the ripple current of the three-phase inductors, instantaneous output power *P*ac from the inverter is given by

$$p_{\mathrm{AC}} = V_{\mathrm{RN}} \cdot I_R \sin^2(\omega_l t + \theta) + V_{\mathrm{SN}} \cdot I_S \sin^2(\omega_l t - 120^\circ + \theta) + V_{\mathrm{TN}} \cdot I_T \sin^2(\omega_l t + 120^\circ + \theta) \quad (1)$$

Where *V*RN, *V*SN, and *V*TN are the amplitudes of the phase voltages; *IR*, *IS* , and *IT* are their current amplitudes; ωl is the line angular frequency; and θ is the phase between ac currents and voltages. If the 3φ power source is unbalanced, there will exist voltage ripple every one-twelfth line period, *Tl* /12, and it can be derived from the following equation:

$$\frac{1}{2}C_{\mathrm{DC}}\left(v_{\mathrm{DC\_MAX}}^2 - v_{\mathrm{DC\_MIN}}^2\right) = \int_0^{\frac{T_l}{12}} (P_{\mathrm{avg}} - p_{\mathrm{AC}})dt \quad (2)$$

Where *v*DC MAX and *v*DC MIN are the peak and valley values of the dc-bus voltage ripple, respectively, and *P*avg is the average power of the inverter input power. Assuming the system is operated in the maximum power rating, 10kW, two of the phase voltages have the maximum and minimum unbalanced variations of 10%. A plot of dc-bus capacitance *C*DC versus dc-bus voltage ripple is illustrated in Fig. 2. It can be seen that when the capacitance is higher than 8 × 470 μF, the voltage ripple is lower than 1V. Therefore, we can select PV capacitor *C*pv = 12 × 470 μF, which is sufficient enough to filter out the ripple effect from the unbalanced grid voltages.

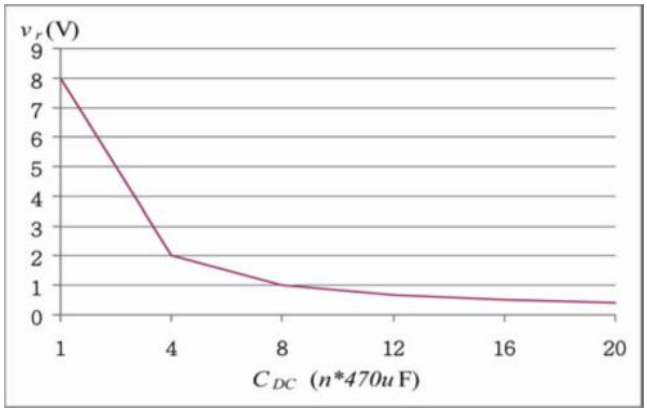

Fig. 2 Plot of dc-bus capacitance *C*DC versus dc-bus voltage ripple *vr* under unbalanced grid voltages

Moreover, there is another voltage ripple effect resulting from non-constant inductors. Assuming the three-phase inductors are identical but with wide inductance variation, the total energy variation will swing at six times line frequency, corresponding to the six-region transitions. The peak-to-peak voltage ripple can be then derived from the following equation:

$$\frac{1}{2}C_{\mathrm{DC}}\left(v_{\mathrm{DC\_MAX}}^2 - v_{\mathrm{DC\_MIN}}^2\right) = \frac{1}{2}\left\{ \left[L_R \cdot i_R^2 + L_S \cdot i_S^2 + L_T \cdot i_T^2\right]_{30^\circ} - \left[L_R \cdot i_R^2 + L_S \cdot i_S^2 + L_T \cdot i_T^2\right]_{0^\circ} \right\}. \quad (3)$$

Fig. 3 shows a plot of *C*DC versus voltage ripple *vr* under the maximum output power of 10 kW and the dc-bus voltage of 380V. It can be observed that *vr* is lower than 0.25V even at only one 470-μF capacitor. Thus, the effect of the voltage ripple due to wide inductance variation is not

significant and can be ignored. However, the capacitor must hold the dc-bus voltage during abrupt power changes, and it will be determined according to energy-storage capability.

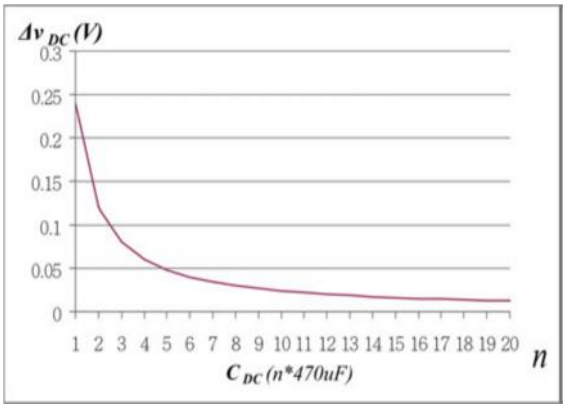

Fig. 3 Plot of dc-bus capacitance *C*DC versus dc-bus voltage ripple *vr* under a maximum output power of 10 kW

2) Energy-Storage Capability: Fig. 4 shows a plot of *C*DC versus dc-bus voltage variation Δ*v*DC under a maximum power change of 10kW and within one-sixth line cycle. For power supply availability, the voltage variation must be lower than 20V (400 –380V or 380–360 V) within one-sixth line cycle, and 12×470-*μ*F capacitance can be selected to fit the appropriate range of dc-bus voltage variation, 10–15V. This set of capacitors was used in the experiment.

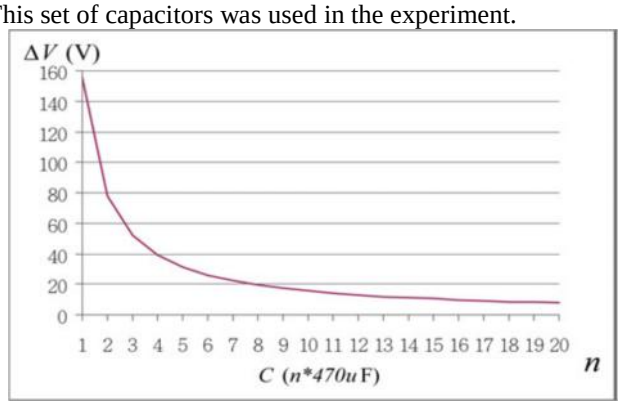

Fig. 4 Plot of dc-bus capacitance *C*DC versus dc-bus voltage variation Δ*v*DC under a 10-kW abrupt change and within one-sixth line cycle

B. Capacitance Estimation

The proposed online capacitance estimation method uses the relationship between dc-bus voltage variation and capacitor current injection, and is based on the capacitor pre-charging circuit. The overall system configuration with a pre-charging circuit is shown in Fig. 5, where the circuit includes a resistor *R* and a relay (normally closed). When any of the three solar arrays generates power, it will charge the dc-bus capacitor through the resistor. The capacitance *C*DC can be then determined as

$$C_{\mathrm{DC}} = \frac{\Delta T}{\Delta v_{\mathrm{DC}}} \cdot i_R \qquad (4)$$

Where Δ*v*DC is the dc-bus voltage variation during time interval Δ*T*, and *iR* is the current through resistor *R*. Since there is no feedback from resistor current *iR*, it is determined as

$$i_R = \frac{(v_{\mathrm{pv}} - v_{\mathrm{DC}})}{R} \qquad (5)$$

Where *V*pv is the solar array voltage. The proposed capacitance estimation is only working during the pre-charging time interval, because the dc distribution system has themerit that all of dc-bus capacitors are installed at the input terminal of the inverter or in a separate box, as shown in Fig. 5. An illustration of the proposed estimation method is shown in Fig. 6. During a sampling period Δ*T*, the estimation equation in (4) can be rewritten as

$$C_{\mathrm{DC}} = \frac{\Delta T}{\Delta v_{\mathrm{DC}}} \cdot i_{R,\mathrm{avg}} = \frac{\Delta T}{v''_{\mathrm{DC}} - v'_{\mathrm{DC}}} \cdot \frac{i'_R + i''_R}{2}$$
$$= \frac{\Delta T}{2R} \cdot \frac{(v''_{\mathrm{pv}} + v'_{\mathrm{pv}}) - (v''_{\mathrm{DC}} + v'_{\mathrm{DC}})}{v''_{\mathrm{DC}} - v'_{\mathrm{DC}}}. \qquad (6)$$

The inverter microcontrollers will feedback the voltages, *v*DC and *v*pv, to determine the dc-bus capacitance from (6). Moreover, the inverter controller will estimate the capacitance automatically when the auxiliary power output is available and the CPU is working. At this moment, the CPU's timer starts to count.

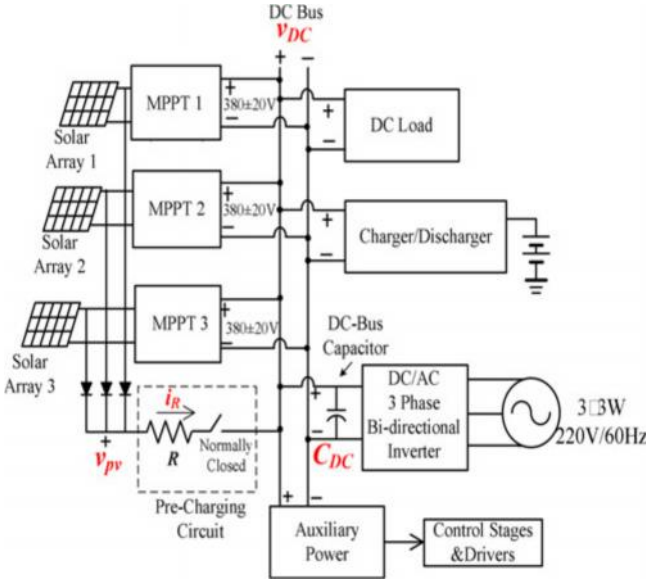

Fig. 5 Configuration of the proposed dc distribution system with a capacitor pre-charging circuit

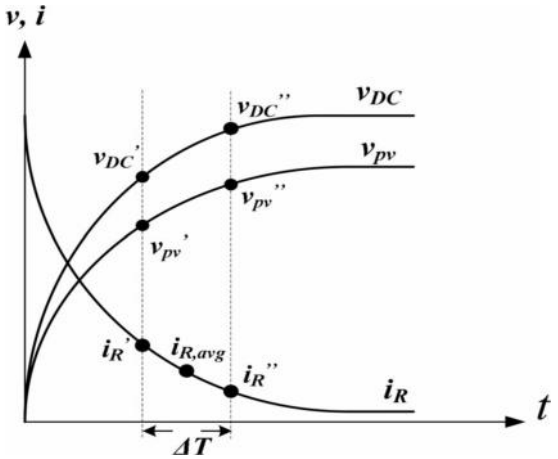

Fig. 6 Illustration of the proposed capacitance estimation method

Although the dc-bus voltage variation Δ*v*DC will change with different start-up times, it does not deteriorate in the estimating results. In the estimation tests, the sampling period Δ*T* was 10ms, resistor *R* = 200 Ω was selected, and four different dc-bus capacitances, 8 × 470, 10 × 470, 12 × 470, and 16 × 470 *μ*F, were, respectively, implemented. A comparison between the estimated and measured data for the different dc-bus capacitances is listed in Table I. The estimation errors are all within 1%, which does not penalize the accuracy of the dc-bus voltage regulation.

TABLE I
COMPARISON BETWEEN MEASURED AND ESTIMATED CAPACITANCES

Measured Values (μF) C_M	Estimated values (μF) C_E	Estimation error (%) $100\%\times(C_M-C_E)/C_M$
3680	3657	0.62
4678	4653	0.53
5573	5539	0.61
7458	7417	0.55

C. DC-BUS VOLTAGE CONTROL

A diagram of the discussed three-phase bidirectional inverter is shown in Fig. 7. It can fit to both delta-connected and Yconnected ac grid. In the designed prototype, *Renesas* microchip *RX*62*T* is adopted for realizing the system controller, which has 1.65 MIPS and includes floating-point calculation and division. By considering wide inductance variation, the inverter can be operated stably, especially in high-current applications. Additionally, the system requires dc-bus voltage control schemes for balancing power flow. It includes linear power management scheme, one line-cycle regulation approach, and one-sixth line cycle regulation approach. A stability analysis is presented to support the proposed regulation approaches.

1. Linear Power Management Scheme

In a system design, the maximum PV power and the maximum dc load power will not exceed the inverter capability. In our developed system, both of the two maximum powers are 10kW. Fig. 8 shows an illustration of the proposed linear power management scheme for achieving a linear relationship between inductor current *iL* and dc-bus voltage *v*DC. The operating range of the dc-bus voltage is 380±20V. When the inverter is operated in grid-connection mode (selling power), the operating range is from 380 to 400V, which ensures an enough voltage level to accommodate abrupt dc load increase. On the other hand, when the inverter is operated in rectification mode (buying power), a lower dc-bus voltage stands for a higher load power. Therefore, in rectification mode, the system does not have extra high enough dc load power to pull the dc-bus voltage below the lower bound. In short, in grid-connection mode, dramatic voltage drop is the major concern when loads are connected to the dc bus, while in rectification mode, sudden voltage jump up is another concern when loads are disconnected from the dc bus.

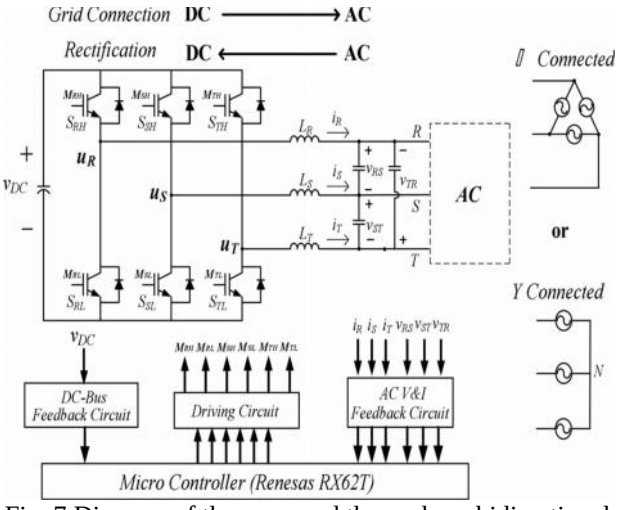

Fig. 7 Diagram of the proposed three-phase bidirectional inverter

Fig. 8 also shows the locus of the dc-bus voltage regulation sequence in grid-connection mode. At time *t*0, the inverter stays at operating point (*v*DC(*n* – 1), *IA*(*n* – 1)) on the load line, where *IA* is the adjustable current command which is tuned every line cycle with the OLCRA. The operating point will move away from the load line to point (*v*DC(*n*), *IA*(*n* – 1)) at *t*1 when there exists power imbalance. Then, the controller will update current command *IA*(*n* – 1) with *IA*(*n*) at the beginning of the *n*th line cycle, which will regulate dc-bus voltage to a new set-point voltage *v*DC(*n* + 1) according to the linear power management scheme. When the inverter reaches operating point (*v*DC(*n*+1), *IA*(*n*)) at *t*2 , the controller will change current command to *IA*(*n* + 1), maintaining dc-bus voltage *v*DC for a new power balance. The system will be operated in the new steady state after time *t*3. The proposed voltage regulation approaches are based on the linear power management scheme and presented in the following section.

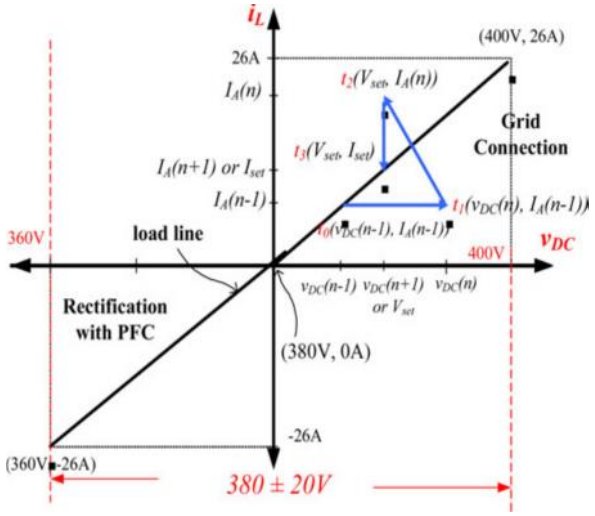

Fig. 8 Illustration of a linear power management scheme for achieving a linear relationship between inductor current *iL* and dc-bus voltage *v*DC

2 One Line-Cycle Regulation Approach

Fig. 9 shows a diagram for illustrating the OLCRA when power imbalance is occurring. In Fig. 9, power imbalance happens at time *tx* 1 , and dc-bus voltage, for

instance, will increase from *v*DC(*n* – 1) to *v*DC(*n*). At time *tn*, dc-bus capacitor current variation Δ*iC* can be determined as

$$\Delta i_C = C_{\mathrm{DC}} \frac{v_{\mathrm{DC}}(n) - v_{\mathrm{DC}}(n-1)}{t_n - t_{x1}}. \quad (7)$$

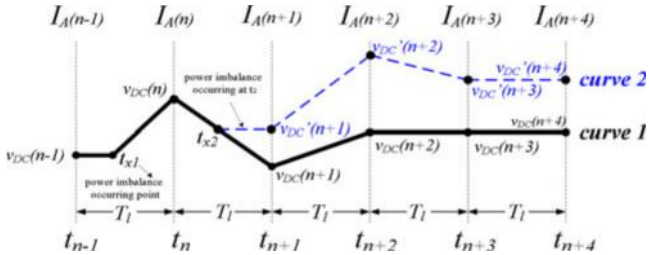

Fig. 9 Illustration of the OLCRA to dc-bus voltage regulation for the dc distribution system with power imbalance

However, time *tx* 1 is unpredictable, and an initial guess is made to *tn*−1 ; thus, new current command *IA*(*n*) for time interval [*tn* , *tn*+1] can be determined based on previous current *IA*(*n* – 1) as

$$I_A(n) = I_A(n-1) + K_{\mathrm{DA}} \Delta i_C - \frac{C_{\mathrm{DC}}\left(v_{\mathrm{DC}}(n+1) - v_{\mathrm{DC}}(n-1)\right)}{T_l} \quad (8)$$

where *Tl* is a line period, *K*DA is a mapping ratio between dc input current and ac output current, which is equal to *v*DC/*V*AC (*V*AC is the RMS value of ac grid voltage, typically 220 V), and the initial current command *IA*(0) is equal to zero at the system start-up. Once the system gets started, current command *IA*(*n* – 1) will be updated cycle by cycle. Voltage *v*DC(*n* + 1) is the set-point voltage, which can be derived based on the relationship shown in Fig. 8, as follows:

$$v_{\mathrm{DC}}(n+1) = 380 + \frac{20\,\mathrm{V}}{26\,\mathrm{A}} \cdot \left(I_A(n-1) + K_{\mathrm{DA}} \frac{C_{\mathrm{DC}}\left(v_{\mathrm{DC}}(n) - v_{\mathrm{DC}}(n-1)\right)}{T_l} \right). \quad (9)$$

In the above equations, *IA*(*n*) is always used for regulating dc-bus voltage to set-point voltage *v*DC(*n* + 1) according to the control diagrams shown in Figs. 8 and 9. The inverter controller will update current command *IA*(*n*) cycle by cycle, that is, *IA*(*i*) will be loaded to *IA*(*I* – 1) after the new current command has been determined at the beginning of a line cycle. In Fig. 9, if another power imbalance occurs at *tx* 2 (curve 2), the inverter will tune current command *IA* continuously to follow curve 2 and reach another set-point.

3. One-Sixth Line-Cycle Regulation Approach

If dc loads change abruptly, the OLCRA cannot regulate dc bus voltage immediately, and it needs a fast dynamic current control to balance the power flow. In a three-phase inverter system, the fast regulation interval is selected to be one-sixth line-cycle according to each zero-crossing point of the three phase line currents. Since the voltage ripple on the dc-bus is insignificant in a three-phase inverter system with even 10% unbalanced three-phase voltage sources, the voltage ripple can be ignored in the control law derivation.

Fig. 10 illustrates the current tuning process of the proposed OSLCRA. With the OSLCRA, the inverter will update current command *IA* at the beginning of each one-sixth line-cycle to drive dc-bus voltage to set-point voltage *v*DC(*n* + 1) at time *tn*+1. Thus, according to a dc-bus voltage variation, the current command control law can be derived as follows:

$$I_A\left(n + \frac{i}{6}\right) = K_{\mathrm{DA}} \frac{6 C_{\mathrm{DC}} \Delta v_i}{T_l} + I_A\left(n + \frac{i-1}{6}\right) \quad (10)$$

where $i = 1, 2, \ldots, 5$, and

$$\Delta v_i = v_{\mathrm{DC}}\left(n + \frac{i}{6}\right) - v_{\mathrm{DC}}\left(n + \frac{(i-1)}{6}\right) - \frac{v_{\mathrm{DC}}(n+1) - v_{\mathrm{DC}}\left(n + \frac{i}{6}\right)}{6 - i} \quad (11)$$

Voltage variation Δ*vi* includes two portions: one is the variation Δ*v*DC(*T*) between two consecutive one-sixth cycles, and the other is the average difference Δ*v*DC(*A*) between *v*DC(*n*+1) and the current operating point:

$$\Delta v_{\mathrm{DC}(T)} = v_{\mathrm{DC}}\left(n + \frac{i}{6}\right) - v_{\mathrm{DC}}\left(n + \frac{(i-1)}{6}\right)$$

And

$$\Delta v_{\mathrm{DC}(A)} = \frac{v_{\mathrm{DC}}(n+1) - v_{\mathrm{DC}}\left(n + \frac{i}{6}\right)}{6 - i}.$$

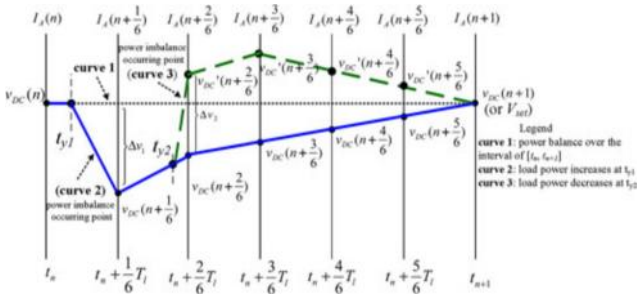

Fig. 10 Illustration of the OSLCRA to dc-bus voltage regulation for the system under power imbalance

The variation Δ*v*DC(*T*) is caused by abrupt power imbalance, of which the dc-bus voltage will deviate from the load line. By adding this variation to the current command in one-sixth cycle, the inverter can balance power flow substantially, but dc-bus voltage *v*DC still does not reach its set-point yet. Thus, the variation Δ*v*DC(*A*) is used for regulating *v*DC to voltage *v*DC(*n* + 1) which has been determined at the beginning of the *n*th line cycle, as shown in (9). With the compensation of these two portions, the dc-bus voltage will come back to the load line after power imbalance occurs at *ty* 1 (curve 2) or *ty* 2 (curve 3), as shown in Fig. 10. It can be observed that the inverter controller updates current command *IA*(*n* + 1/6) at *tn* + T*l* /6 after dc-bus voltage drops abruptly at *ty* 1 (curve 2). However, the inverter controller will determine a wrong current command due to the unpredictable time *tY* 1 , and

ISSN 2321-6905

the dc-bus voltage will not be regulated to a correct voltage value until next one-sixth line cycle, *tn* + 2*Tl*/6. If another power imbalance occurs at *ty* 2 (curve 3), the same regulation process will be conducted again. That is, the inverter will use a correct current command *IA*(*n* + 3/6) to regulate the dc-bus voltage to a set-point voltage. Furthermore, current command *IA*(*n*) must be modified for determining command *IA*(*n* + 1) at the beginning of a new cycle due to the one-sixth line-cycle command change, and it is just equal to the average value of all current commands within the time interval of [*tn* , *tn*+1]. The determination of current command *IA*(*n*) can be expressed as

$$I_A(n) = \frac{I_A(n-1) + \sum_{i=1}^{5} I_A\left(n + \frac{i}{6}\right)}{6}. \qquad (12)$$

III. SIMULATION RESULTS

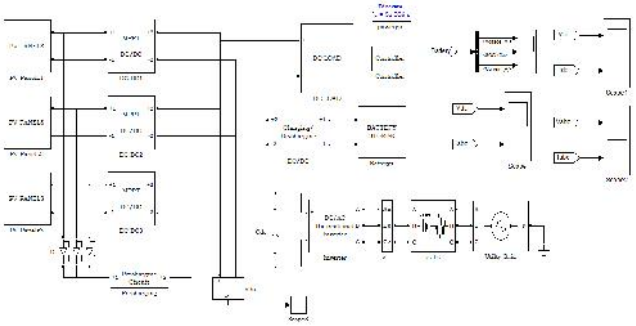

Fig 11 simulation diagram of proposed system

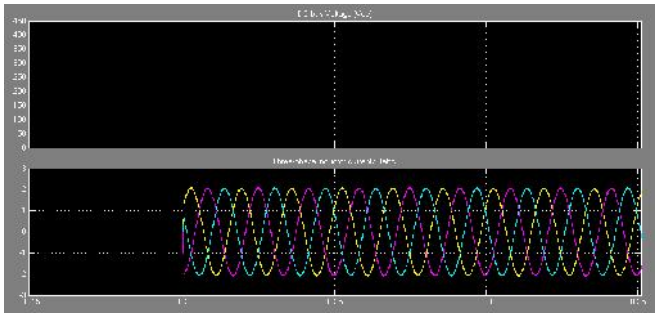

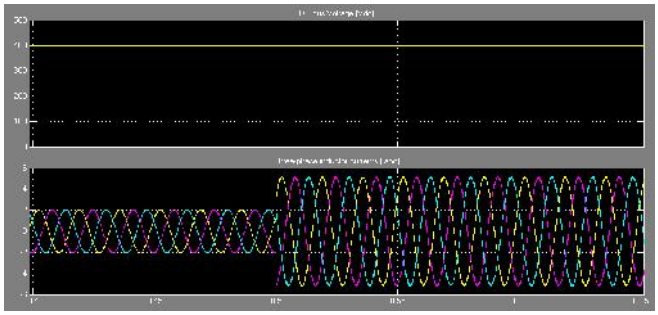

Fig. 11.Measured waveforms of the three-phase inductor currents and dc-bus voltage *v*DC for dc load variation (a) from no load to 800Wand (b) from 800W to 2 kW in rectification mode with BSS

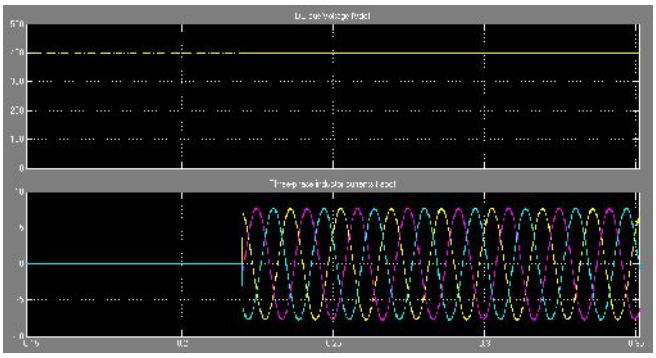

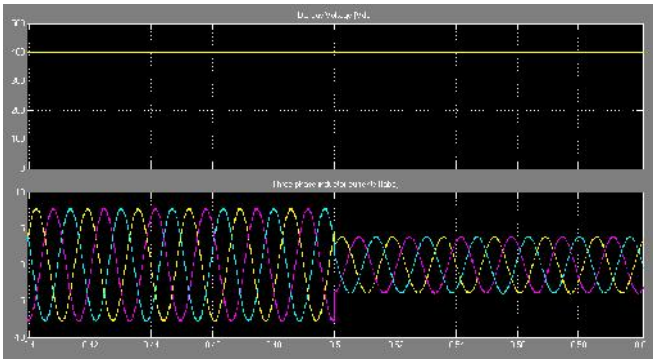

Fig. 12 Measured waveforms of the three-phase inductor currents and dc-bus voltage *v*DC for dc load variation (a) from no load to 3kW and (b) from 3 to 1.5 kW in rectification mode with BSS

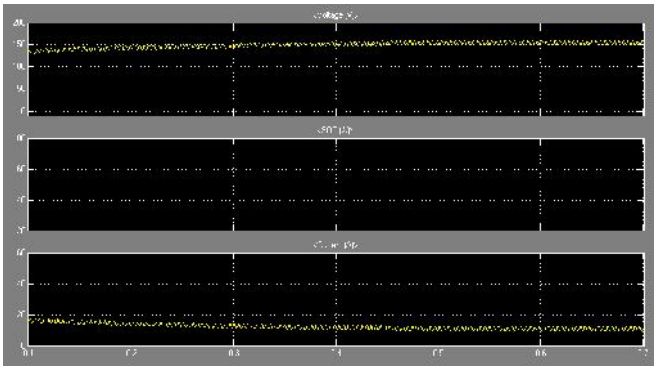

Fig 13 measured waveforms of BSS

CONCLUSION

A dc-bus voltage control for three-phase bidirectional inverters in dc distribution systems has been presented. The linear power management scheme including both grid-connection and rectification modes have been described in detail. In the paper, the one line-cycle regulation approach based on the linear power management scheme has been proposed for tuning current command cycle by cycle to regulate the dc-bus voltage according to the load line. For an abrupt voltage change, the one-sixth line cycle regulation approach has been also proposed to prevent over/under dc-bus voltage fault, ensuring system availability. Since both of the approaches are dependent on the parameter of dc-bus capacitance, a determination of capacitor size and a capacitance estimation method have been discussed according to the aspects of dc-bus voltage ripple and energy-storage capability.

REFERENCES

[1] T.-F. Wu, K.-H. Sun, C.-L. Kuo, and C.-H. Chang, "Predictive current controlled 5-kW single-phase bidirectional inverter with wide inductance variation for dc-microgrid applications," *IEEE Trans. Power Electron.*, vol. 25, no. 12, pp. 3076–3084, Dec. 2010.

[2] L. Xu and D. Chen, "Control and design of a DC microgrid with variable generation and energy storage," *IEEE Trans. Power Del.*, vol. 26, no. 4, pp. 2513–2522, Oct. 2011.

[3] Z.-H. Ye, D. Boroyevich, K. Xing, and F.-C. Lee, "Design of parallel sources in DC distributed power systems by using gain-scheduling technique," in *Proc. IEEE Power Electron. Spec. Conf.*, Aug. 1999, pp. 161–165.

[4] Y. Ito, Y. Zhongqing, and H. Akagi, "DC microgrid based distribution power generation system," in *Proc. IEEE Int. Power Electron. Motion Control Conf.*, Aug. 2004, pp. 1740–1745.

[5] J. M. Guerrero, J. C. Vasquez, J. Matas, L. G. D. Vicuna, and M. Castilla, "Hierarchical control of droop-controlled AC and DC microgrid—A general approach toward standardization," *IEEE Trans. Ind. Electron.*, vol. 58, no. 1, pp. 158–172, Jan. 2011.

[6] H. Kakigano, A. Nishino, and T. Ise, "Distributed voltage control for DC microgrid with fuzzy control and gain-scheduling control," in *Proc. IEEE Int. Conf. Power Electron.*, 2011, pp. 256–263.

[7] H.Kakigano,Y. Miura, and T. Ise, "Low-voltage bipolar-type dc microgrid for super high quality distribution," *IEEE Trans. Power Electron.*, vol. 25, no. 12, pp. 3066–3075, Dec. 2010.

[8] J.-S. Park, J.-K. Choi, B.-G. Gu, I.-S. Jung, E.-C. Lee, and K.-S. Ahn, "Robust DC-Link voltage control scheme for photovoltaic power generation system PCS," in *Proc. IEEE Int. Telecommun. Energy Conf.*, Oct. 2009, pp. 1–4.

[9] D. Salomonsson, L. Soder, and A. Sannino, "An adaptive control system for a DC microgrid for data centers," *IEEE Trans. Ind. Appl.*, vol. 44, no. 6, pp. 1910–1917, Nov./Dec. 2008.

[10] J.-S. Park, J.-K. Choi, B.-G. Gu, I.-S. Jung, E.-C. Lee, and K.-S. Ahn, "A hybrid renewable DC microgrid voltage control," in *Proc. IEEE Int. Power Electron. Motion Control Conf.*, May 2009, pp. 725–729.

[11] Z. Li, T. Wu, X. Yan, K. Sun, and J. M. Gurrero, "Power control of DC microgrid using DC bus signaling," in *Proc. IEEE Appl. Power Electron. Conf.*, Mar. 2011, pp. 1926–1932.

[12] A. Engler, "Applicability of droops in low voltage grids," *Int. J. Distrib. Energy Res.*, vol. 1, no. 1, pp. 1–5, Jan. 2005.

[13] J. A. Restrepo, J. M. Aller, A. Bueno, J. C. Viola, A. Berzoy, R. Harley, and T. G. Habetler, "Direct power control of a dual converter operating as a synchronous rectifier," *IEEE Trans. Power Electron.*, vol. 26, no. 5, pp. 1410–1417, May 2011.

[14] M. G. Molina and P. E. Mercado, "Power flow stabilization and control of microgrid with wind generation by superconducting magnetic energy storage," *IEEE Trans. Power Electron.*, vol. 26, no. 3, pp. 910–922, Mar. 2011.

[15] Y. C. Chang and C. M. Liaw, "Establishment of a switched-reluctance generator-based common DC microgrid system," *IEEE Trans. Power Electron.*, vol. 26, no. 9, pp. 2512–2527, Sep. 2011.

[16] N. Hur, J. Jung, and K. Nam, "A fast dynamic DC-link power-balance scheme for a PWM converter-inverter system," *IEEE Trans. Ind. Electron.*, vol. 48, no. 4, pp. 794–1803, Aug. 2001.

[17] J. Yao, H. Li, Y. Liao, and Z. Chen, "An improved control strategy of limiting the DC-link voltage fluctuation for a doubly fed induction wind generator," *IEEE Trans. Power Electron.*, vol. 23, no. 3, pp. 1205–1213, May 2008.

[18] T.-F. Wu, L.-C. Lin, C.-H. Chang, Y.-L. Lin, and Y.-C. Chang, "Current improvement for a3 bi-directional inverter with wide inductance variation," in *Proc. IEEE ECCE Asia*, May/Jun. 2011, pp. 1777–1784.

[19] E. Aeloiza, J.-H. Kim, P. Enjeti, and P. Ruminot, "A real time method to estimate electrolytic capacitor condition in PWM adjustable speed drives and uninterruptible power supplies," in *Proc. IEEE Power Electron. Spec. Conf.*, Jun. 2005, pp. 2867–2872.

[20] A.-G. Abo-Khalil and D.-C. Lee, "DC-link capacitance estimation in AC/DC/AC PWM converters using voltage injection," *IEEE Trans. Ind. Appl.*, vol. 44, no. 5, pp. 1631–1637, Sep. 2008.

[21] A. J. Roscoe, S. J. Finney, and G. M. Burt, "Tradeoffs between AC power quality and DC bus ripple for 3-Phase 3-wire inverter-connected devices within microgrids," *IEEE Trans. Power Electron.*, vol. 26, no. 3, pp. 674– 688, Mar. 2011.

[22] G. Petrone, G. Spagnuolo, and M. Vitelli, "Optimization of perturb and observe maximum power point tracking method," *IEEE Trans. Power Electron.*, vol. 20, no. 4, pp. 963–973, Jul. 2005.

[23] A. Khaligh, C. H. Rivetta, and G. A. Williamson, "Constant power loads and negative impedance instability in automotive systems: Definition, modeling, stability, and control of power electronic converters and motor drives," *IEEE Trans. Veh. Technol.*, vol. 55, no. 4, pp. 1112–1125, Jul. 2006.

[24] P. Liutanakul, A. Awan, S. Pierfederici, B. Nahid-Mobarakey, and F. Meibody-Tabar, "Linear stabilization of a DC bus supplying a constantpower load," *IEEE Trans. Power Electron.*, vol. 25, no. 2, pp. 475–488, Feb. 2010.

[25] A. Kwasinski and C. N. Onwuchekwa, "Dynamic behavior and stabilization of DC microgrids with instantaneous constant-power loads," *IEEE Trans. Power Electron.*, vol. 26, no. 3, pp. 822–834, Mar. 2011.